

The Dimeric “Hand-Shake” Motif in Complexes and Metallo–Supramolecular Assemblies of Cyclotrimeratrylene-Based Ligands

Christopher Carruthers,^[a] Tanya K. Ronson,^[a] Christopher J. Sumby,^[a, b]
Aleema Westcott,^[a] Lindsay P. Harding,^[c] Timothy J. Prior,^[d, e] Pierre Rizkallah,^[d] and
Michaele J. Hardie*^[a]

Abstract: A series of clathrate and metal complexes with cyclotrimeratrylene-like molecular host ligands show a similar dimeric homomeric inclusion motif in which a ligand arm of one host is the intra-cavity guest of another and vice versa. This “hand-shake” motif is found in the trinuclear transition metal complex $[\text{Cu}_3\text{Cl}_6(\mathbf{1})]\cdot\text{CH}_3\text{CN}\cdot 1.5\text{H}_2\text{O}$ in which **1** is tris(4-[2,2',6',2'']-terpyridyl)-benzyl)cyclotriguaiacylene; in the self-

included M_4L_4 tetrahedral metallo-supramolecular assembly $[\text{Ag}_4(\mathbf{2})_4]\cdot(\text{BF}_4)_4$ in which **2** is tris-(2-quinolylmethyl)cyclotriguaiacylene; in the 1D coordination chains $[\text{Ag}(\mathbf{4})]\cdot\text{ReO}_4$

$\cdot\text{CH}_3\text{CN}$ and $[\text{Ag}(\mathbf{5})]\cdot\text{SbF}_6\cdot 3\text{DMF}\cdot\text{H}_2\text{O}$ in which **4** is tris(1H-imidazol-1-yl)-cyclotriguaiacylene and **5** is tris{4-(2-pyridyl)benzyl}cyclotriguaiacylene; and in the acetone clathrate of tris{4-(2-pyridyl)benzyl-amino}cyclotriguaiacylene. Clathrates of ligands **2** and **5** do not show the same dimeric motif, although **2** has an extended homomeric inclusion motif that gives a hexagonal network.

Keywords: coordination chains • cyclotrimeratrylene • host–guest chemistry • supramolecular chemistry • tetrahedral assembly

Introduction

Cyclotrimeratrylene (CTV) is a molecular host with a relatively rigid shallow bowl-shaped cavity.^[1] Recent interest in CTV chemistry includes applications in liquid crystals,^[2] gas-

binding^[3] and organometallic cryptophanes,^[4] organo-gels,^[5] anion sensing,^[6] fullerene separations^[7] and in metallo-supramolecular assemblies.^[8–12] Like all molecular hosts, CTV contains an intrinsic molecular cavity that can bind other molecular species to form host–guest complexes. In general, clathrate complexes of CTV with small organic guests form homomeric mis-aligned stacking motifs^[13] and the intra-cavity complexation of a small organic guest molecule is somewhat rarer.^[14] Both CTV and its chiral analogue cyclotriguaiacylene (CTG) can be converted into extended-arm host molecules through functionalisation at the upper rim. In their simple crystalline clathrate complexes these also tend to form homomeric inclusion associations, including four reported examples of a dimeric clasping or “hand-shake” motif in which an arm of one molecule extends into the molecular cavity of the other and vice versa, as shown diagrammatically in Scheme 1.^[9,15,16] The same dimeric motif has also been reported for calix[4]- and calix[5]arenes.^[17] Dimerisation usually occurs around a centre of inversion to give dimers in the case of the chiral CTG analogues. A similar homomeric inclusion motif which extends to a 1D chain has also been reported for CTV analogues^[9,18] and *p*-tert-butyl-calix[5]arene.^[19] Other homomeric inclusion motifs involving molecular hosts include self-inclusion, in which the guest fragment is covalently attached to the host frag-

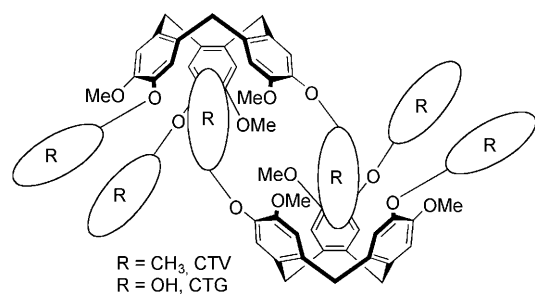
[a] C. Carruthers, Dr. T. K. Ronson, Dr. C. J. Sumby, Dr. A. Westcott, Dr. M. J. Hardie
School of Chemistry
University of Leeds
Woodhouse Lane, Leeds, LS2 9JT (UK)
Fax: (+44) 113-343-6565
E-mail: m.j.hardie@leeds.ac.uk

[b] Dr. C. J. Sumby
Present address: School of Chemistry and Physics
The University of Adelaide
North Terrace, Adelaide, SA 5005 (Australia)

[c] Dr. L. P. Harding
Department of Chemical and Biological Sciences
University of Huddersfield
Huddersfield, HD1 3DH (UK)

[d] Dr. T. J. Prior, Dr. P. Rizkallah
STFC Daresbury Laboratory
Daresbury, Warrington, WA4 4AD (UK)

[e] Dr. T. J. Prior
Present address: Department of Chemistry
University of Hull
Kingston upon Hull, HU6 7RX (UK)



Scheme 1. Cartoon showing a "hand-shake" dimer formed between two generic CTG-derived molecular hosts.

ment,^[20] and head-to-tail inclusion^[20] motifs leading to polymeric assemblies.^[21,22]

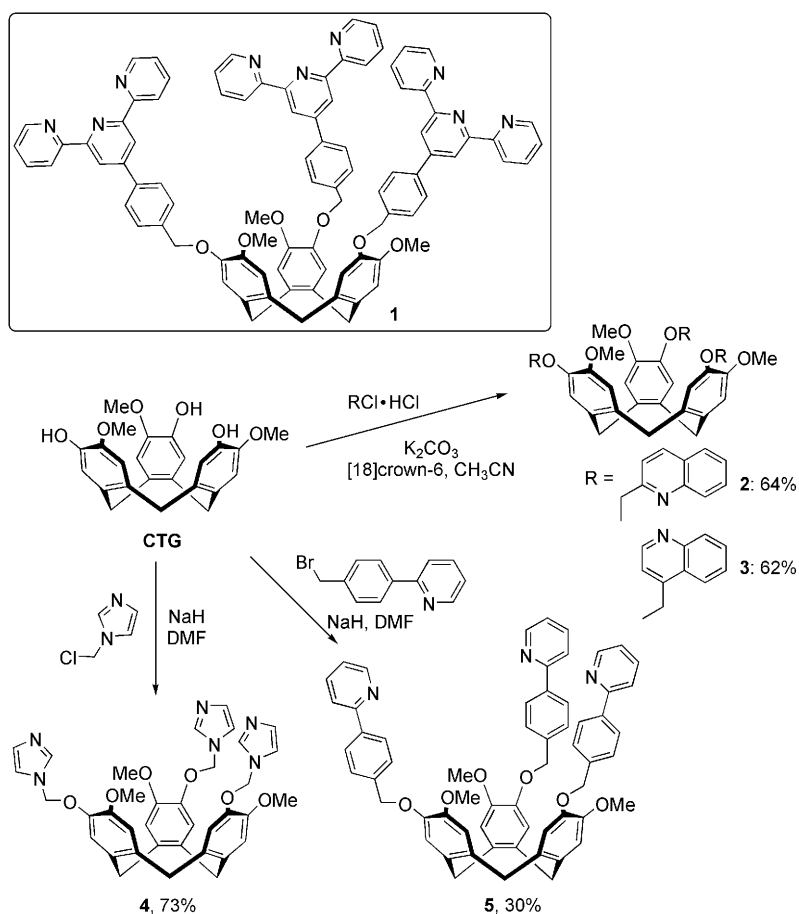
Our major interest in CTV chemistry is in exploiting the pyramidal shape of CTG extended-arm hosts as ligands for discrete metallo-supramolecular prisms and/or coordination polymers with transition metals. Following on from Shinkai's earlier report of $[M_3L_2]$ capsules involving CTV-type ligands,^[8] we have reported a $[Ag_2L_2]^{2+}$ capsule,^[9] a $[M_3L_2]_2$ [2]catenane,^[11] a $[Ag_4L_4]^{4+}$ star-burst tetrahedron^[9,10] and a $[Pd_6L_8]^{12+}$ stella octangula,^[12] along with 1D, 2D and 3D coordination polymers.^[9,23] We report herein a series of metal complexes with CTG-based ligands that exhibit the dimeric "hand-shake" motif. These include a discrete trinuclear complex which is dimeric in nature in both solid and solution states; an unusual M_4L_4 metallo-supramolecular assembly in which the hand-shake interaction results in a tightly packed assembly with no significant internal space; and 1D coordination polymers.

Results and Discussion

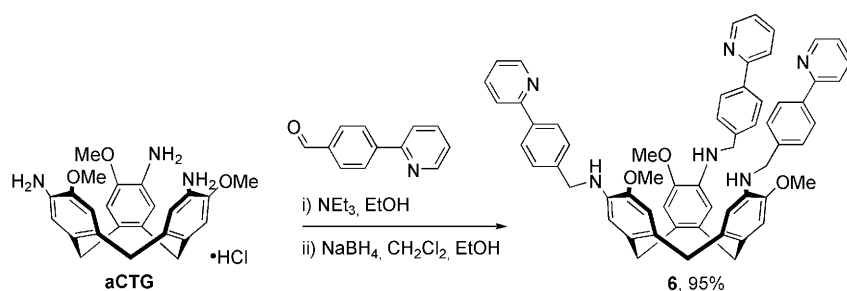
Ligand synthesis: The synthesis of tris(4-[2,2',6',2''-terpyridyl]-benzyl)cyclotriguaiacylene **1** has been previously reported.^[15] Tris-(2-quinolylmethyl)cyclotriguaiacylene **2** and tris-(4-quinolylmethyl)cyclotriguaiacylene **3** were synthesised by reaction of cyclotriguaiacylene (CTG) with the appropriate chloromethyl-quinoline hydrochloride in the presence of base and [18]crown-6 in acetonitrile at reflux, Scheme 2. The synthesis of tris(1H-imidazol-1-yl)cyclotriguaiacylene **4** and tris[4-(2-pyridyl)benzyl]cyclotriguaiacy-

lene **5** required the use of more forcing conditions with reaction in dry dimethylformamide (DMF) with NaH as base, Scheme 2. Tris[4-(2-pyridyl)benzyl-amino]cyclotriguaiacylene **6** was synthesised in two steps from the hydrochloride salt of the precursor 3,8,13-triamino-2,7,12-trimethoxy-10,15-dihydro-5H-tribenzo[*a,d,g*]cyclononene (aCTG),^[24] with initial formation of the imine through reaction with 4-(2-pyridyl)benzaldehyde followed by reduction with sodium borohydride, Scheme 3.

Discrete metal complexes and related ligand clathrates: Reaction of $CuCl_2$ with the terpyridyl-derived ligand **1** in acetonitrile under solvothermal conditions results in the isolation of green crystals of complex $[Cu_3Cl_6(1)] \cdot CH_3CN \cdot 1.5H_2O$ **7**. The crystals were extremely small and their structure was determined using synchrotron radiation. $[Cu_3Cl_6(1)]$ is a discrete trinuclear complex with Cu^{II} centres bound at each terpyridyl arm of the ligand. The asymmetric unit of the crystal structure comprises one complete trinuclear complex along with solvent acetonitrile and water positions. All three Cu^{II} coordination spheres are similar, each with a distorted square pyramidal geometry from a chelating terpyridyl group and terminal Cl^- ligands in the apical and one basal site (Figure 1). In the case of Cu_3 , the basal Cl is approximately coplanar with the 3N-plane of the terpyridyl group,



Scheme 2. Ligand **1** (box) and synthesis of ligands **2–5**.



Scheme 3. Synthesis of ligand 6.

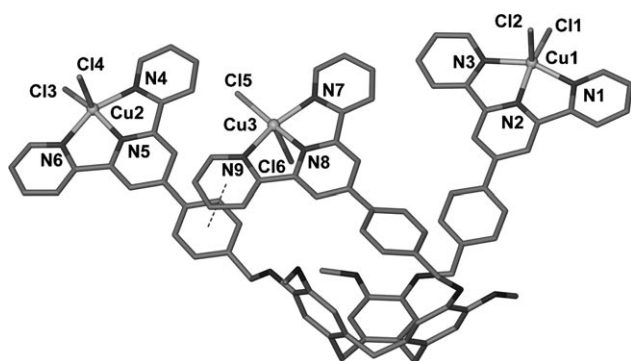


Figure 1. Trinuclear $[Cu_3Cl_6(1)]$ species from the crystal structure of $[Cu_3Cl_6(1)] \cdot CH_3CN \cdot 1.5H_2O$. Intramolecular π - π stacking interaction is shown as dashed line. Selected bond lengths [Å] and angles [°]: Cu1–N1 2.062(8), Cu1–N2 1.955(7), Cu1–N3 2.049(8), Cu1–Cl1 2.250(2); Cu1–Cl2 2.434(3), Cu2–N4 2.039(9), Cu2–N5 1.942(7), Cu2–N6 2.052(9), Cu2–Cl3 2.254(3), Cu2–Cl4 2.415(9), Cu3–N7 2.075(10), Cu3–N8 1.922(10), Cu3–N9 2.077(9), Cu3–Cl5 2.206(4), Cu3–Cl6 2.647(4); N2–Cu1–Cl1 154.9(2), N1–Cu1–Cl1 99.5(2), N3–Cu1–Cl1 98.7(2), N2–Cu1–Cl2 99.3(2), N3–Cu1–Cl2 96.7(2), N1–Cu1–Cl2 93.3(2), Cl1–Cu1–Cl2 105.80(10), N5–Cu2–Cl3 153.3(2), N4–Cu2–Cl3 98.4(2), N6–Cu2–Cl3 98.8(3), N5–Cu2–Cl4 99.6(2), N4–Cu2–Cl4 96.9(3), N6–Cu2–Cl4 92.4(3), Cl3–Cu2–Cl4 107.07(12), N8–Cu3–Cl5 172.2(3), N7–Cu3–Cl5 100.3(4), N9–Cu3–Cl5 99.0(3), N8–Cu3–Cl6 85.7(3), N7–Cu3–Cl6 89.9(3), N9–Cu3–Cl6 99.2(2), Cl5–Cu3–Cl6 102.15(16).

whereas for Cu1 and Cu2 it is below the 3N-plane. The orientation of the benzyl-terpyridyl- $CuCl_2$ arms is quite distinct for each group. In one case it is approximately coplanar with its associated guaiacol group, another is twisted around its CH_2-C_{phenyl} bond putting the benzyl-terpyridyl fragment approximately perpendicular to the guaiacol. For the third group (of Cu3), rotation has occurred around the $O-CH_2$ bond, which folds the benzyl-terpyridyl- $CuCl_2$ fragment inwards such that it forms an intramolecular face-to-face π - π stacking interaction with the benzyl-terpyridyl- $CuCl_2$ fragment of Cu2 at an aryl ring centroid separation of 3.54 Å (Figure 1). The orientation of the Cu3 coordination sphere is inverted with respect to the other two, and this unusual orientation of one of the extended arms forces one of the neighbouring methoxy groups of the ligand to be bent about 60° away from the adjoining aromatic ring.

A handful of discrete coordination and organometallic complexes of CTV- or aCTG-based ligands have been previously reported,^[25–27] including trinuclear complexes with Ag^I ,

Ni^{II} , Cu^{II} , Pt^{II} or Pd^{II} .^[26,27] There are only two crystal structures of prior examples of simple trinuclear coordination complexes,^[26] and in both cases the extended metallated arms of the complexes point outwards from the CTG-bowl in a symmetric or near symmetric fashion. This is not the case in complex 7 in which the asymmetric conformation produces an extended host with a C-shaped cavity or

cleft in the solid state. This conformation allows the trinuclear $[Cu_3Cl_6(1)]$ complexes to form dimers with the “handshake” motif. The benzyl-terpyridyl- $CuCl_2$ arm of Cu3 of one complex within the dimer occupies the molecular cavity of the other and vice versa, giving a racemic dimer (Figure 2). There are no π - π stacking interactions between the two complexes within a dimer. In the extended structure columns of dimers form along the crystallographic *c*-axis through extensive π - π stacking interactions. These interactions occur between the benzyl-terpyridyl- $CuCl_2$ arms of Cu1 and Cu2 at aryl ring centroid separations ranging from

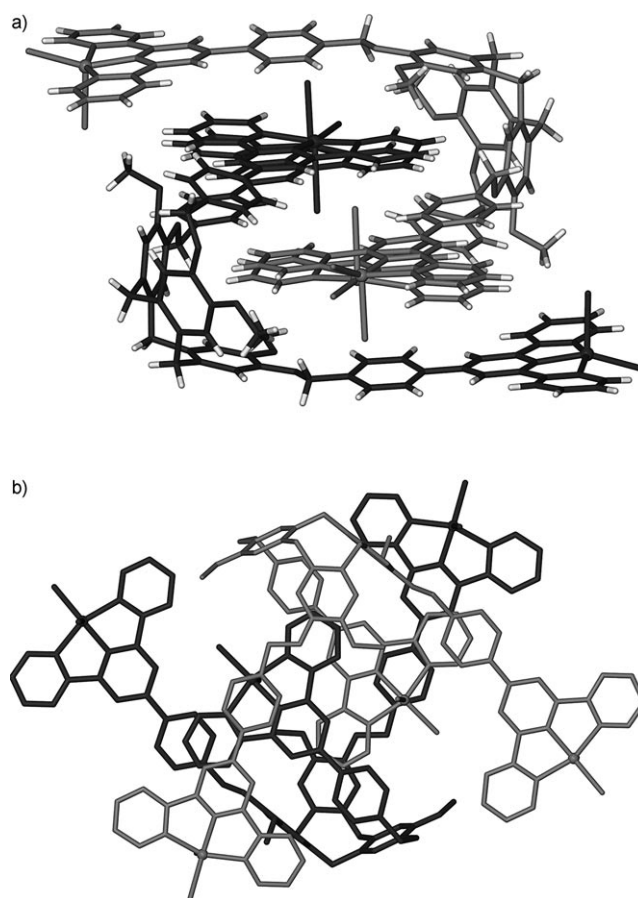


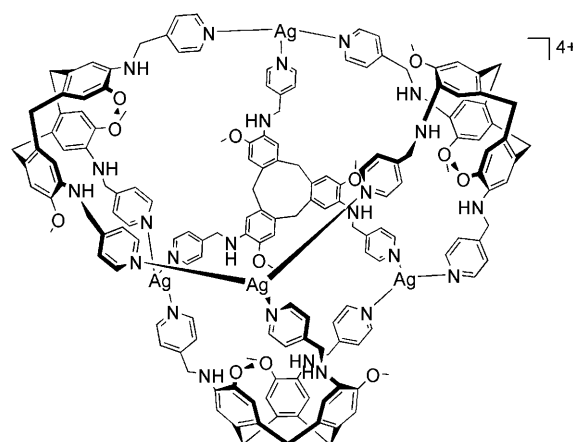
Figure 2. Two views of the homomeric handshake dimer of complex $[Cu_3Cl_6(1)]$ from the crystal structure of $[Cu_3Cl_6(1)] \cdot CH_3CN \cdot 1.5H_2O$.

3.58 to 3.82 Å. Similar solid-state self-complementary dimerisation of coordination complexes with molecular clefts have been reported by Steel and co-workers,^[28] and Bosnich and co-workers.^[29] Both examples are dinuclear with the complexes adopting a C-shaped conformation, and, like $[\text{Cu}_3\text{Cl}_6(\mathbf{1})]$, the latter example also involves terpyridyl coordinating groups.

Electrospray mass spectrometry (ES-MS) studies indicate that the trinuclear $[\text{Cu}_3\text{Cl}_6(\mathbf{1})]$ complex exists in solution, and that dimerisation of the complexes occurs in solution as well as in the solid state. An overlapping $1+2+$ peak at $m/z:1739.16$ corresponds to a single trinuclear complex $[\text{Cu}_3\text{Cl}_5(\mathbf{1})]^+$ and the dimeric species $\{[\text{Cu}_6\text{Cl}_{10}(\mathbf{1})_2]\}^{2+}$ (calcd 1739.89); there is a further peak corresponding to the single complex $[\text{Cu}_3\text{Cl}_4(\mathbf{1})]^{2+}$ at $m/z:852.11$ (calcd 853.56). Within the mass spectrometer, the $[\text{Cu}_3\text{Cl}_6(\mathbf{1})]$ complexes fragment through the loss of a single benzyl-terpyridyl- CuCl_2 arm. Remarkably, this does not lead to the dissociation of the dimer and peaks occur for the loss of one arm from one complex of the dimer and for the loss of two arms from the dimer; namely at $m/z:1512.16$ corresponding to $[\text{Cu}_5\text{Cl}_8(\mathbf{1})(\mathbf{1}-\text{C}_{22}\text{H}_{16}\text{N}_3)]^{2+}$ (calcd 1512.08) and an overlapping signal at $m/z:1283.18$ for $[\text{Cu}_4\text{Cl}_6(\mathbf{1}-\text{C}_{22}\text{H}_{16}\text{N}_3)_2]^{2+}$ and the single complex $[\text{Cu}_2\text{Cl}_3(\mathbf{1}-\text{C}_{22}\text{H}_{16}\text{N}_3)]^{2+}$ (calcd 1283.71). From inspection of Figure 2b of the crystal structure, it is evident that the hand-shake dimer could lose a single benzyl-terpyridyl- CuCl_2 arm, or indeed one such arm from each complex, and still retain its integrity as a dimer. Notably, the analogous dimers of Steel^[28] and Bosnich^[29] are both shown to dissociate in solution.

A tetrahedral metallo-supramolecular assembly is afforded by reaction of tris-(2-quinolylmethyl)cyclotriguaniacylene **2** with AgBF_4 in $\text{CF}_3\text{CH}_2\text{OH}$. Complex $[\text{Ag}_4(\mathbf{2})_4]\cdot(\text{BF}_4)_4$ **8** is isolated as small single crystals. The single crystal X-ray structure of $[\text{Ag}_4(\mathbf{2})_4]\cdot(\text{BF}_4)_4$ reveals that the complex is a discrete $[\text{Ag}_4\text{L}_4]^{4+}$ tetrahedral metallo-supramolecular assembly, but one that is structurally quite distinct from the previously reported “star-burst” $[\text{Ag}_4\text{L}_4]^{4+}$ assembly (L = tris(4-pyridylmethylamino)cyclotriguaniacylene).^[9,10] The structure of $[\text{Ag}_4(\mathbf{2})_4]^{4+}$ is complicated and easiest to understand by comparison with the simpler star-burst assembly, which is shown diagrammatically in Scheme 4. The star-burst assembly is an M_4L_4 tetrahedron with metal centres at the corners of the tetrahedron and ligands (L) taking up the facial positions. There have only been a relatively small number of tetrahedral M_4L_4 assemblies reported with tripodal ligands (L).^[9,10,30–32]

The asymmetric unit of $[\text{Ag}_4(\mathbf{2})_4]\cdot(\text{BF}_4)_4$ consists of one ligand, one Ag^{I} centre and one BF_4^- counter-anion. The ligand is asymmetric with all three quinoline arms having different orientations. The Ag^{I} centres have linear geometry with $\text{Ag}-\text{N}$ distances 2.205(10) and 2.169(10) Å and $\text{N}-\text{Ag}-\text{N}$ angle 176.0(4)°. In complex **8** the four crystallographically equivalent Ag^{I} centres of the $[\text{Ag}_4(\mathbf{2})_4]^{4+}$ assembly are arranged in a distorted tetrahedron with respect to one another at $\text{Ag}\cdots\text{Ag}$ separations 9.31 and 10.34 Å (Figure 3). This compares with shorter typical $\text{Ag}\cdots\text{Ag}$ separations of $\approx 8.7-$



Scheme 4. Schematic diagram of the “star-burst” $[\text{Ag}_4\text{L}_4]^{4+}$ tetrahedral metallo-supramolecular assembly.

10.1 Å for structures of the star-burst $[\text{Ag}_4\text{L}_4]^{4+}$ assembly.^[9,10] Whereas in the star-burst tetrahedron the Ag centres form the corners of tetrahedron and each ligand forms a face of the tetrahedron coordinating to three Ag^{I} centres, for complex **8** each ligand only coordinates to two Ag^{I} centres with only two of the three quinoline arms coordinating. Furthermore, for the star-burst assembly, the basal $(\text{CH}_2)_3$ plane of the ligand is coplanar with the Ag_3 face of the tetrahedron; here the ligand is twisted away from alignment with the tetrahedron’s face. This twisting occurs to accommodate the coordination geometry of the ligand and the dimeric homomeric motif formed by the ligands. The dimeric motif involves a quinoline arm of one ligand acting as the intracavity guest for the other ligand and vice versa, Figure 3a. The guest quinoline arm is not positioned directly over the centre of the host ligand’s cavity, but rather positioned to one side where it forms a $\pi-\pi$ stacking interaction with one of the host ligand’s quinoline arms at an aryl centroid separation of 3.49 Å. The two ligands involved in this “hand-shake” motif are both of the same enantiomer and are not linked together through metal coordination. The formation of a chiral hand-shake is quite unusual, with all other examples involving a racemic pair of ligands. There are two such hand-shake ligand pairs in the $[\text{Ag}_4(\mathbf{2})_4]^{4+}$ assembly, and the ligands in the second pair are of the opposite enantiomer. The two sets of ligand pairs are linked together by coordinating to the Ag^{I} centres, to give the $[\text{Ag}_4(\mathbf{2})_4]^{4+}$ assembly (Figure 3b). The non-coordinating quinoline group of each ligand forms $\pi-\pi$ stacking interactions with one of the coordinating quinolines of another ligand (aryl centroid separation 3.490 Å) and its C_6 aryl ring is positioned above a Ag^{I} centre, effectively blocking the metal centre from any further coordination interactions. The closest $\text{Ag}\cdots\text{C}$ separation to this quinoline is 3.48 Å, which is too long to indicate the presence of an organometallic interaction.

There is no significant internal space within the $[\text{Ag}_4(\mathbf{2})_4]^{4+}$ assembly. In contrast, most other examples of M_4L_4 assemblies, including, the “star-burst” tetrahedron, do

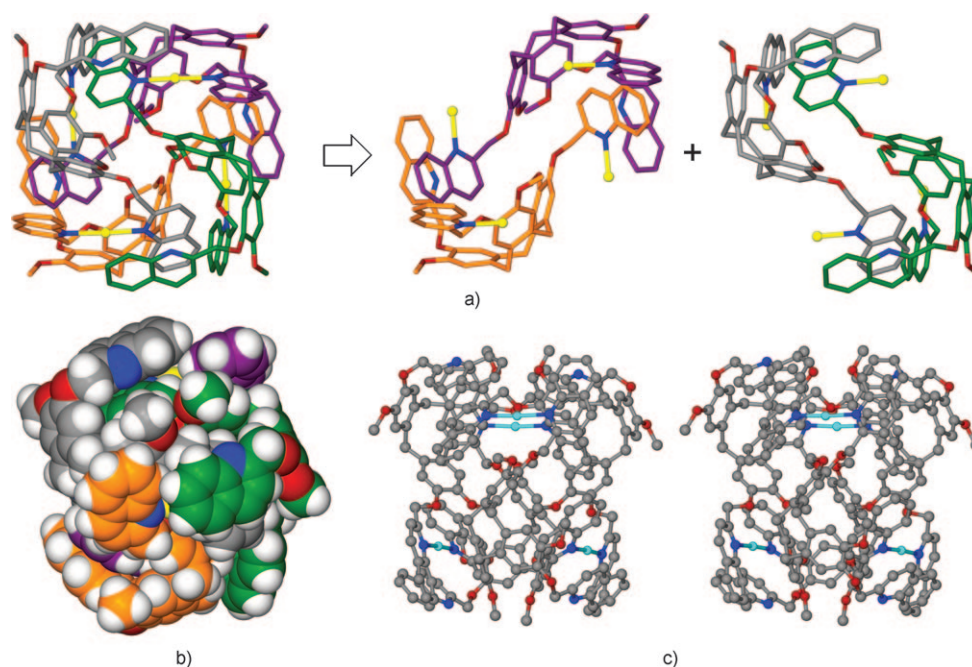


Figure 3. Views of the $[\text{Ag}_4(\mathbf{2})_4]^{4+}$ assembly: a) and b) are from the crystal structure of complex **8**, with each ligand shown in a different colour scheme, in which a) shows the $[\text{Ag}_4(\mathbf{2})_4]^{4+}$ cage (left) and an exploded view (right) highlighting the two pairs of hand-shake ligand dimers; and b) gives a space-filling view of the $[\text{Ag}_4(\mathbf{2})_4]^{4+}$ assembly. c) Is a ball-and-stick stereo-view of the $[\text{Ag}_4(\mathbf{2})_4]^{4+}$ assembly.

possess sufficient space to act as supramolecular hosts.^[9,10,30,32] A further exception to this is a series of complexes reported by Raymond and co-workers,^[32] which feature small internal cavities owing to the relatively small size of the tripodal ligands used. In most cases however, cationic or anionic guests are encapsulated inside the tetrahedral assemblies,^[30] and exchange of cationic guests has been reported.^[31]

In the crystal lattice of **8** the $[\text{Ag}_4(\mathbf{2})_4]^{4+}$ assemblies do not approach each other closely and each $[\text{Ag}_4(\mathbf{2})_4]^{4+}$ assembly is surrounded by six BF_4^- anions in a distorted hexagonal pattern. The crystalline material is likely to be highly solvated, but the quality of the X-ray data obtained does not allow for this to be elucidated. The solvent-accessible void within the crystal lattice is calculated to be approximately 25% of the unit cell volume.^[33]

On titrating AgBF_4 into a solution of ligand **2** in $\text{CF}_3\text{CD}_2\text{OD}$ at room temperature the ^1H NMR signal of the ligand broadens considerably, indicating the formation of a solution phase species that is undergoing fast exchange on the NMR timescale. The spectrum begins to sharpen at lower temperatures, but, unfortunately, has not sufficiently sharpened at the freezing limit of the solvent to allow for identification of any solution species. There is no significant change to the room temperature ^1H NMR signal of the ligand when AgBF_4 is added in the coordinating solvent CD_3CN . It is also notable that 1:1 mixtures of AgBF_4 and **2** in 2,2,2-trifluoroethanol sometimes results in the formation of a gel, and that crystals were isolated after using an excess of metal salt. ES-MS studies do not give any evidence of the $[\text{Ag}_4(\mathbf{2})_4]^{4+}$ tetrahedron, with the highest observed m/z

value of 1965.50 corresponding to a dimeric $[\text{Ag}_2(\mathbf{2})_2](\text{BF}_4)^+$ species (calcd 1966.44).

The crystal structure of a clathrate complex of ligand **2**, obtained by its recrystallisation from 2,2,2-trifluoroethanol, also displays a homomeric inclusion motif, but one that is quite distinct from the dimeric hand-shake motif. The asymmetric unit of the structure of complex $\mathbf{2}\cdot\text{H}_2\text{O}\cdot 4\text{CF}_3\text{CH}_2\text{OH}$ **9** is shown in Figure 4a. The ligand within complex **9** has non-crystallographic C_3 symmetry with all three quinoline arms emanating directly outwards from the CTG framework. Each quinoline forms hydrogen bonding interactions with water or 2,2,2-trifluoroethanol at $\text{N}\cdots\text{O}$ separations ranging from 2.77 to 2.78 Å, Figure 4a. Each ligand acts as a host for three other crystallographically equivalent ligands, with a single quinoline arm of each of the “guest” ligands directed into the molecular cavity (Figure 4b). Two of the three guest quinoline arms show π - π stacking interactions at an aryl ring centroid separation of 3.65 Å. The orientation of the “guest” ligand **2** molecules is inverted with respect to that of the host ligand, hence these homomeric associations generate a 2D network of ligands. Each ligand also forms face-to-face π - π stacking interactions to three other ligands through its exo surface, at aryl centroid separations ranging from 3.49 to 3.97 Å. The extensive π - π stacking and host-guest interactions create an overall 3D extended network of ligands with large channels running along the c axis. The channels contain solvent water and $\text{CF}_3\text{CH}_2\text{OH}$ molecules (Figure 5).

The previously reported isomer of ligand **2**, tris-(8-quinolymethyl)cyclotriguaiacylene, forms an acetonitrile clathrate complex that displays the dimeric hand-shake motif.^[15] A

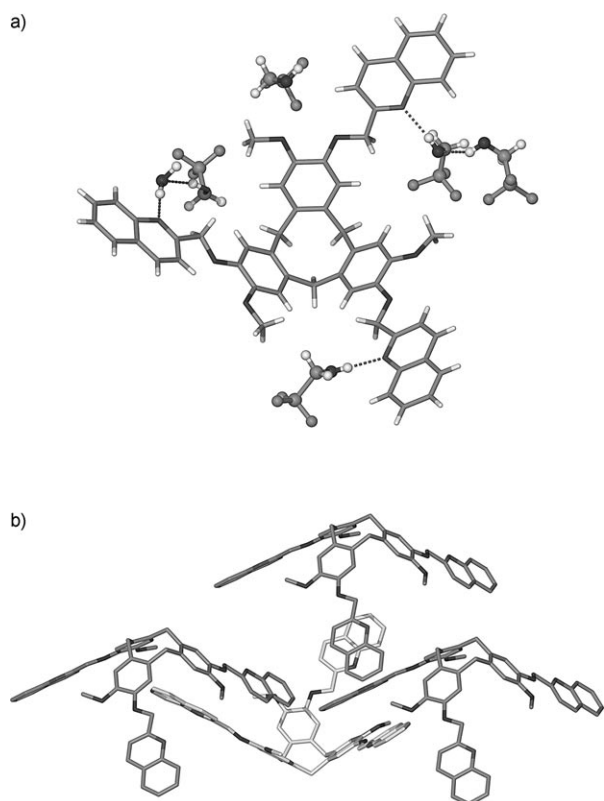


Figure 4. Crystal structure of $2 \cdot \text{H}_2\text{O} \cdot 4 \text{CF}_3\text{CH}_2\text{OH}$ **9**. a) The asymmetric unit with hydrogen bonds indicated as dashed lines; b) An illustration of the three homomeric associations of the ligand with the "host" ligand shown in lighter shading.

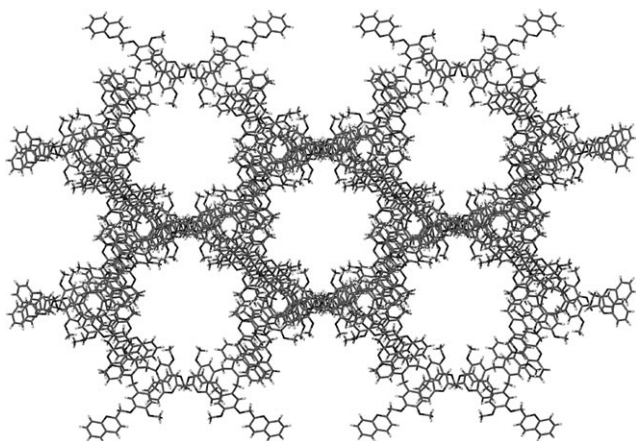


Figure 5. Extended packing diagram for complex **9** viewed down the c axis with solvent molecules excluded.

new isomer of **2**, ligand tris-(4-quinolylmethyl)cyclotrignaiacylene **3**, also forms an acetonitrile clathrate as complex $3 \cdot \text{CH}_3\text{CN}$ **10**, but one in which the crystal structure shows a different type of association between the ligands. Ligand **3** in complex **10** has C_1 symmetry and one upper rim methyl group is significantly rotated away with a $\text{CO} \cdots \text{O}$ angle of 89° between the methoxy group and O-methylquinoline. A

linear chain of ligands is formed through host-guest associations (Figure 6). Only one of the three quinoline arms is involved in this interaction. The linear chain motif found here

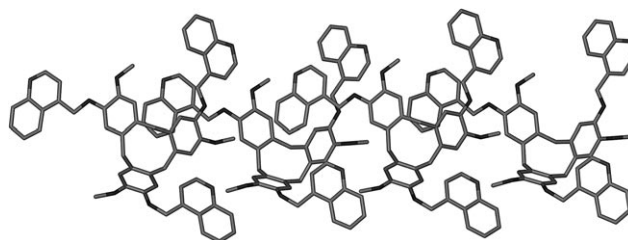


Figure 6. Section of the crystal packing diagram of complex $3 \cdot \text{CH}_3\text{CN}$ **10** showing the formation of a head-to-tail inclusion chain.

is more akin to linear head-to-tail associations of functionalised calixarenes^[21] than other reported 1D inclusion chains of CTG-derivatives. Examples of the latter usually involve a mis-aligned self-stacking giving a zig-zag rather than a linear chain.^[18] There are face-to-face π - π stacking interactions between quinoline groups of different inclusion chains of complex **10** at a ring centroid separation of 3.89 \AA , as well as between quinoline and core benzene groups at a ring centroid separation of 3.81 \AA .

Polymeric metal complexes and related ligand clathrates:

Complexes $[\text{Ag}(\mathbf{4})] \cdot \text{ReO}_4 \cdot \text{CH}_3\text{CN}$ **11**, and $[\text{Ag}(\mathbf{5})] \cdot \text{SbF}_6 \cdot 3 \text{DMF} \cdot \text{H}_2\text{O}$ **12** were isolated from reaction of their respective ligands with Ag^{I} salts. Both complexes show topologically identical coordination chains that incorporate dimeric homomeric inclusion motifs. The crystal structures of both complexes are of low symmetry with a metal cation, anion, complete ligand and solvent positions comprising the asymmetric units. In both cases, the orientation of the ligand side-arms is asymmetric. One of the pyridyl groups and most of the solvent DMF molecules of $[\text{Ag}(\mathbf{5})] \cdot \text{SbF}_6 \cdot 3 \text{DMF} \cdot \text{H}_2\text{O}$ were modelled as disordered.

The Ag^{I} cation of $[\text{Ag}(\mathbf{4})] \cdot \text{ReO}_4 \cdot \text{CH}_3\text{CN}$ has a T-shaped geometry, being coordinated by imidazole groups from three different, though crystallographically equivalent, ligands. Each ligand bridges between three crystallographically equivalent Ag^{I} centres to create a polymeric complex (Figure 7a). The polymer is a snaking 1D chain with ladder-like topology, with both the ligand and metal acting as a 3-connecting centre. The $[\text{Ag}(\mathbf{5})]^+$ chain within the complex $[\text{Ag}(\mathbf{5})] \cdot \text{SbF}_6 \cdot 3 \text{DMF} \cdot \text{H}_2\text{O}$ is topologically identical to that of the $[\text{Ag}(\mathbf{4})]^+$ chain, although the geometry around the Ag^{I} centre is quite different. Here, the Ag^{I} has a distorted geometry closer to trigonal than T-shaped, with coordination by three pyridyl groups of different ligands and one bond length much longer than the others, Figure 7b. The $[\text{Ag}(\mathbf{5})]^+$ 1D coordination chain is considerably straighter than that seen for $[\text{Ag}(\mathbf{4})]^+$ (Figure 7).

For both $[\text{Ag}(\mathbf{4})]^+$ and $[\text{Ag}(\mathbf{5})]^+$ the orientation of the molecular cavities of the ligands alternates along the chain and each ligand is involved in one pairwise host-guest inter-

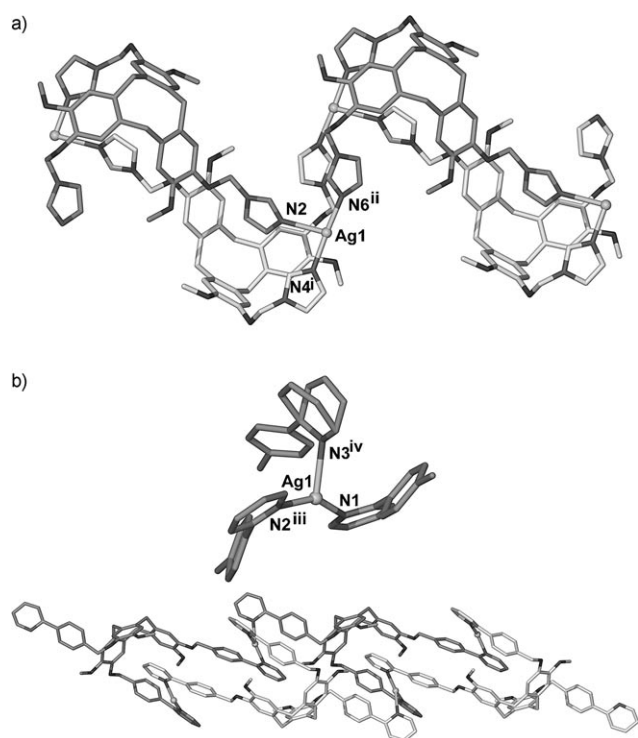


Figure 7. Coordination chains with homomeric pair-wise inclusion motifs between the ligands. Each ligand within a pair is shown with different shading. a) $[\text{Ag}(\mathbf{4})]^+$ chain from the crystal structure of $[\text{Ag}(\mathbf{4})]\cdot\text{ReO}_4\cdot\text{CH}_3\text{CN}$ **11**; b) From the crystal structure of $[\text{Ag}(\mathbf{5})]\cdot\text{SbF}_6\cdot 3\text{DMF}\cdot\text{H}_2\text{O}$ **12**: Ag^{I} coordination sphere and pyridyl disorder (top) and $[\text{Ag}(\mathbf{5})]^+$ chain (bottom, with only one disorder fragment shown for clarity). Selected bond lengths [Å] and angles [°]: complex **11**: Ag1-N2 2.607(4); Ag1-N4^{i} 2.140(3); $\text{Ag1-N6}^{\text{ii}}$ 2.133(3); $\text{N2-Ag1-N4}^{\text{i}}$ 86.24(13); $\text{N2-Ag1-N6}^{\text{ii}}$ 98.91(13); $\text{N4}^{\text{i}}\text{-Ag1-N6}^{\text{ii}}$ 171.25(14); complex **12**: Ag1-N1 2.229(6); $\text{Ag1-N2}^{\text{iii}}$ 2.246(6); $\text{Ag1-N3}^{\text{iv}}$ 2.505(7); $\text{N1-Ag1-N2}^{\text{iii}}$ 150.6(2); $\text{N1-Ag1-N3}^{\text{iv}}$ 113.3(2); $\text{N2}^{\text{iii}}\text{-Ag1-N2}^{\text{iv}}$ 95.9(3). Symmetry operations: i: 2-X, 2-Y, 1-Z; ii: X, 1+Y, Z; iii: 1-X; -Y; -Z; iv: 1+X, Y, 1+Z.

action across an inversion centre with one other ligand. This takes the form of the familiar hand-shake motif. In $[\text{Ag}(\mathbf{4})]^+$ the guest imidazole group is oriented such that it forms a single $\text{C-H}\cdots\pi$ edge-to-face interaction with a guaicol moiety of the host fragment ($\text{C-H}\cdots\text{ring}$ centroid distance 2.46 Å at 153.6° at H, $\text{C}\cdots\text{ring}$ centroid separation 3.34 Å). In $[\text{Ag}(\mathbf{5})]^+$ face-to-face $\pi\text{-}\pi$ stacking interactions occur between the guaicol host and pyridyl guest fragments at a ring centroid separation of 3.56 Å, and between the linking benzyl groups at 3.97 Å between the aryl ring centres. This chain topology along with the same inclusion motif has been observed once before within a coordination chain involving a CTG-related ligand, in the chain structure of $[\text{Ag}(\text{H}_2\text{O})\text{L}]^+$ in which $\text{L} = \text{tris}(3\text{-pyridylmethyl-amino})\text{cyclotri-guaiacylene}$.^[9] In that case the Ag^{I} had tetrahedral geometry with a terminal aquo ligand and bridging L ligands.

The snaking, zig-zagging shape of the $[\text{Ag}(\mathbf{4})]^+$ chain within $[\text{Ag}(\mathbf{4})]\cdot\text{ReO}_4\cdot\text{CH}_3\text{CN}$ leads to an interesting packing motif whereby channels are formed along the crystallographic *a*-axis. The chains stack in an aligned fashion along

the *a* axis and form face-to-face $\pi\text{-}\pi$ stacking interactions between chains in the *bc* plane at an aryl centroid distance 3.80 Å. The channels contain well-ordered ReO_4^- anions and solvent acetonitrile (Figure 8). Each ReO_4^- anion forms a weak interaction to the exposed face of a Ag^{I} cation at $\text{Re-O}\cdots\text{Ag}$ separation 2.91 Å.

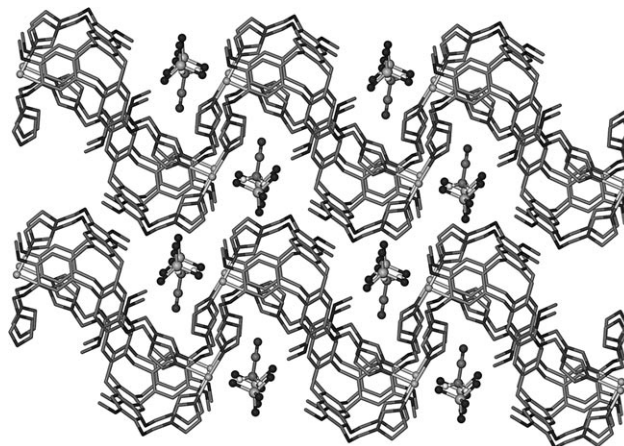


Figure 8. Packing diagram for the crystal structure of complex **9** shown slightly displaced from the *a* axis.

A simple clathrate complex of ligand **4** has yet to be isolated, however a clathrate of ligand **5**, complex **5**·DMF·0.25 CH_3OH , **13**, can be isolated by recrystallisation of the ligand from a methanol-DMF mixture. The asymmetric unit of the crystal structure of **13** is shown in Figure 9,

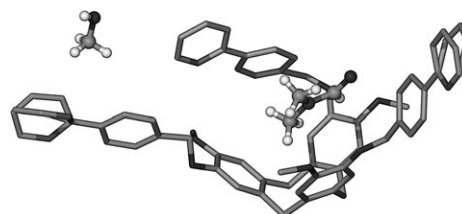


Figure 9. Asymmetric unit of the crystal structure of **5**·DMF·0.25 CH_3OH **13** illustrating the intra-cavity DMF guest complexation, and disorder of the pyridyl groups. Hydrogen atoms are excluded from ligand **5** for clarity.

and comprises a complete molecule of each of the components. The orientation of each (2-pyridyl)benzyl side-arm within ligand **5** are all distinct and two pyridyl groups show disorder. The DMF is the intra-cavity guest for the host ligand thus excluding the possibility of forming dimeric hand-shake inclusion motifs between the ligands. As expected, a hydrophobic methyl group of the guest DMF is oriented into the hydrophobic cavity of the ligand. Examples of intra-cavity guest complexation with CTV or simple extended-arm CTV complexes are relatively limited. There are no face-to-face $\pi\text{-}\pi$ stacking interactions within the extended lattice of **13**.

Although ligand **5** does not show the hand-shake motif in a simple clathrate complex, the closely related ligand **6**—with an amine link to the (2-pyridyl)benzyl group in place of the ether link of **5**—does form a clathrate complex with the dimeric hand-shake motif. The acetone clathrate of ligand **6**, complex **6**·2 CO(CH₃)₂, **14**, has the given composition as the asymmetric unit. All three (2-pyridyl)benzyl arms show a different orientation, and a racemic dimer is formed across an inversion centre whereby a (2-pyridyl)benzyl arm of one ligand is oriented into the molecular cavity of the other and vice versa (Figure 10). Acetone guest molecules occupy clefts within the dimer. Reaction of ligand **6** with a variety of metal salts did not lead to the isolation of any metal complexes, and the reaction mixture discoloured indicating decomposition of the ligand.

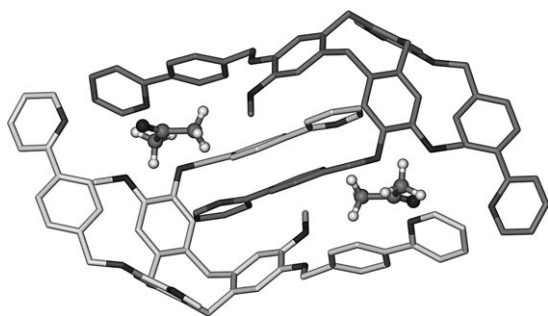


Figure 10. View from the crystal structure of **6**·2 CO(CH₃)₂ **14** showing the formation of a “hand-shake” dimer and position of one acetone guest. The two symmetry related ligands have different shading. Only the major disorder positions are shown and hydrogen atoms have been excluded from **6** for clarity.

Conclusion

The dimeric association of two molecular hosts had been previously observed for a small number of cycotrivenatrylene-based and calixarene molecular hosts. This inclusion motif has been shown to also be exhibited by different types of metal complexes of CTV-type ligands, including a discrete trinuclear complex, metallo-supramolecular tetrahedron and 1D coordination polymers. The interaction is sufficiently robust that it can be observed by mass spectrometry even with fragmentation of the coordination complex. The two pairs of metal connected hand-shake dimers of [Ag₄(**2**)₄]⁴⁺ lead to a very unusual self-included tetrahedral prism with no significant internal space. These results indicate that in future studies of discrete and polymeric metallo-supramolecular species featuring CTV-derived host ligands, simultaneous prevention of the two common modes of CTV inclusion will have to be investigated to enable the full realization of the host cavity for inclusion of other entities. Upper rim functionalization with large metal coordinating groups, as described here, generally limits the aligned and misaligned stacking of the CTV core moieties commonly seen for the parent molecular hosts CTV and CTC, but engages this second “hand-shake” motif of inclusion. This could be ac-

complished by appending more hydrophilic metal binding arms to the CTV to minimize inclusion by a second host cavity.

Experimental Section

Cyclotriguiacylene,^[34] tris(4-[2,2',6',2''-terpyridyl]benzyl)cyclotriguiacylene,^[15] 3,8,13-triamino-2,7,12-trimethoxy-10,15-dihydro-5*H*-tribenzo[*a,d,g*]cyclononene hydrochloride (aCTG.3HCl),^[24] 1-chloromethylimidazole hydrochloride,^[35] and 4-bromomethyl-2-phenylpyridine^[36] were synthesised by literature methods.

Synthesis

Tris-(2-quinolylmethyl)cyclotriguiacylene 2: Cyclotriguiacylene (216 mg, 0.52 mmol), potassium carbonate (777 mg, 5.6 mmol) and [18]crown-6 (62 mg, 0.25 mmol) were stirred together at reflux in acetonitrile (40 mL) under nitrogen for 30 minutes. 2-(Chloromethyl)quinoline monohydrochloride (389 mg, 1.8 mmol) was then added and the mixture heated at reflux under nitrogen for 24 h. After this time another 3 equivalents of the quinoline salt was added and heating at reflux was continued until NMR monitoring indicated that the reaction was complete (a further 48 h). Water (50 mL) was then added, precipitating the product, which was collected, washed with methanol (20 mL) then diethyl ether (10 mL) and dried under vacuum to give **2** (280 mg, 64%), as a white solid. m.p. 110–114°C; ¹H NMR (300 MHz, CDCl₃) δ=3.27 (s, 9H; O-CH₃), 3.35 (d, *J*=13.8 Hz, 3H; CH₂), 4.60 (d, *J*=13.8 Hz, 3H; CH₂), 5.41 (s, 6H; CH₂-O), 6.47 (s, 3H; Ar CH), 6.78 (s, 3H; Ar CH), 7.55 (t, *J*=7 Hz, 3H; quin.H9) 7.6 (d, *J*=8 Hz, 3H; quin.H3), 7.75 (t, *J*=7 Hz 3H; quin.H8), 7.83 (d, *J*=8 Hz, 3H; quin.H10), 8.06 (d, *J*=8.5 Hz, 3H; quin.H4), 8.13 ppm (d, *J*=8.5 Hz, 3H; quin.H7); ¹³C NMR (75 MHz, CDCl₃) δ=36.5, 55.6, 72.4, 113.3, 115.0, 118.9, 126.5, 127.7, 127.9, 128.8, 129.8, 131.5, 132.5, 137.1, 146.6, 147.6, 148.0, 158.7 ppm; ES-MS: *m/z*: 832.3353 [M+H⁺] C₅₄H₄₆N₃O₆⁺ requires 832.9597; elemental analysis calcd (%) for C₅₄H₄₅N₃O₆·5H₂O: C 70.3, H 6.0, N 4.6; found C 70.4, H 5.7, N 4.3.

Tris-(4-quinolylmethyl)cyclotriguiacylene 3: A similar procedure to the synthesis of **2** was employed using 4-(chloromethyl)quinoline monohydrochloride (300 mg, 1.4 mmol). NMR monitoring indicated that the reaction required 72 h of heating at reflux after the second addition of quinoline salt. Compound **3** was isolated as a white solid (251 mg, 62%). m.p. 136–140°C; ¹H NMR (300 MHz, CDCl₃) δ=3.43 (d, *J*=13.8 Hz, 3H; CH₂), 3.55 (s, 9H; O-CH₃), 4.68 (d, *J*=13.8 Hz, 3H; CH₂), 5.58 (dd, ⁴*J*_{HH}=26.9 Hz, ²*J*_{HH}=14.3 Hz, 6H; CH₂O), 6.58 (s, 3H; Ar CH), 6.81 (s, 3H; Ar CH), 7.54 (d, *J*=4.3 Hz, 3H; quin.H3) 7.59 (t, *J*=7.5 Hz, 3H; quin.H9), 7.76 (t, *J*=7.3 Hz, 3H; quin.H8), 7.96 (d, *J*=8.3 Hz, 3H; quin.H10), 8.18 (d, *J*=8.3 Hz, 3H; quin.H7), 8.89 ppm (d, *J*=4.4 Hz, 3H; quin.H2); ¹³C NMR (75 MHz, CDCl₃) δ=36.8, 56.4, 69.2, 114.1, 117.3, 119.4, 123.1, 126.0, 127.3, 129.8, 130.8, 132.1, 133.9, 142.9, 147.0, 149.5, 149.2, 150.9 ppm; ES-MS: *m/z*: 832.4562 [M+H⁺] C₅₄H₄₆N₃O₆⁺ requires 832.9597; elemental analysis calcd (%) for C₅₄H₄₅N₃O₆·H₂O: C 76.3, H 5.6, N 4.9; found C 76.4, H 5.5, N 4.9.

Tris(1*H*-imidazol-1-yl)cyclotriguiacylene 4: NaH (60% dispersion in mineral oil, 390 mg, 9.75 mmol) was added in small portions to a solution of CTG (200 mg, 0.490 mmol) in dry DMF (7 mL) and the mixture stirred for 30 min. Solid 1-chloromethylimidazole hydrochloride (600 mg, 3.92 mmol) was added and the mixture stirred at room temperature for 48 h. Water (100 mL) and CH₂Cl₂ (100 mL) were added and the aqueous layer washed with CH₂Cl₂ (2×100 mL). The combined organic layers were washed with water (5×100 mL), dried (MgSO₄) and evaporated in vacuo. The residue was purified by column chromatography (alumina, 5% MeOH in CH₂Cl₂) to afford **4** as an off-white powder (232 mg, 73%). m.p. 149–153°C; ¹H NMR (500 MHz, CDCl₃) δ=3.40 (d, *J*=13.8 Hz, 3H; CH₂), 3.84 (s, 9H; CH₃), 4.59 (d, *J*=13.8 Hz, 3H; CH₂), 5.71 (m, 6H; CH₂-O), 6.68 (s, 3H; aryl CH), 6.63 (s, 3H; aryl CH), 6.98 (s, 3H; imidazole CH), 7.02 (s, 3H; imidazole CH), 7.49 ppm (s, 3H; imidazole CH); ¹³C NMR (75 MHz, CDCl₃) δ=36.6, 56.4, 114.3, 119.6, 123.5, 130.3, 131.9, 136.9, 138.1, 143.6, 150.4 ppm; ES-MS: *m/z*: 649

[*M+H*⁺]; elemental analysis calcd (%) for C₃₆H₃₆N₆O₆·H₂O: C 64.85, H 5.74, N 12.61; found C 65.20, H 5.65, N 12.65.

Tris(4-(2-pyridyl)benzyl)cyclotriuaicylene 5: A similar procedure to the synthesis of **4** was employed using CTG (200 mg, 0.5 mmol), NaH (60% dispersion in mineral oil, 200 mg, 8 mmol) and 4-bromomethyl-2-phenylpyridine (610 mg, 2.45 mmol). The crude product was purified by column chromatography on silica gel using 0.5% methanol in dichloromethane as an eluent. The off-white solid obtained was suspended in diethyl ether to give **5** as an off-white solid (130 mg, 30%). m.p. 173–176 °C; ¹H NMR (500 MHz, CDCl₃): δ = 3.48 (d, *J* = 13.5 Hz, 3H; CH₂), 3.62 (9H; s, OMe), 4.67 (d *J* = 13.5 Hz, 3H; CH₂), 5.17 (s, 6H; OCH₃), 6.64 (s, 3H; aryl H), 6.82 (s, 3H; aryl H), 7.22 (t, *J* = 4.8 and 5.1 Hz 3H; H5), 7.5 (d, *J* = 8 Hz, 6H; benzyl H), 7.73 (m, 6H; H3, H4), 7.9 (d, *J* = 8 Hz, 6H; benzyl H), 8.68 ppm (d, *J* = 4.6 Hz, 3H; H6); ¹³C NMR (75 MHz, CDCl₃): δ = 36.9, 56.5, 71.7, 114.1, 116.5, 120.8, 122.6, 127.5, 132.0, 133.0, 137.2, 138.9, 139.3, 147.4, 148.8, 150.1, 157.3 ppm; ES-MS: *m/z*: 910.4 [*M*⁺]; elemental analysis calcd (%) for C₆₀H₅₁O₆N₃·1.5H₂O: C 76.89; H 5.82 N 4.48; found C 76.90, H 5.7, N 4.30.

Tris(4-(2-pyridyl)benzyl-amino)cyclotriuaicylene 6: aCTG·3HCl (518 mg, 1.01 mmol), 4-(2-pyridyl)benzaldehyde (570 mg, 3.11 mmol), triethylamine (2 mL) and ethanol (50 mL) were heated at reflux for 3 h. The reaction mixture was cooled to room temperature, the solvent removed in vacuo to give a bright yellow solid. This was dissolved in a 1:1 mixture of dichloromethane and ethanol (40 mL), sodium borohydride (460 mg, 12.1 mmol) was added in small portions and the reaction mixture stirred at room temperature for 72 h. The solvent was removed in vacuo and the solid taken up in dichloromethane (150 mL), the chlorinated extract washed with water (50 mL) and then dried over magnesium sulfate. The solvent was removed and the resulting oily solid triturated with ethanol. The resulting pale yellow solid was collected, washed with ethanol, then ether, and dried under vacuum to give **6** (869 mg; 95%). m.p. 146–148 °C; ¹H NMR (500 MHz, CDCl₃) δ = 3.37 (d, *J* = 13.7 Hz, 3H; CH₂), 3.51 (s, 9H; OCH₃), 4.38 (m, 6H; NHCH₂py), 4.67 (d, *J* = 13.7 Hz, 3H; CH₂), 4.64 (bs, 3H; NH), 6.47 (s, 3H; aryl CH), 6.50 (s, 3H; aryl CH), 7.22 (t, *J* = 5.0 Hz, 3H; H5), 7.46 (d, *J* = 8.1 Hz, 6H; benzyl H), 7.73 (m, 6H; H3 and H4), 7.95 (d, *J* = 8.2 Hz, 6H; benzyl H), 8.54 ppm (d, *J* = 4.7 Hz, 3H; H6); ¹³C NMR (75 MHz, CDCl₃) δ = 36.5, 48.1, 55.4, 111.2, 111.3, 120.3, 122.0, 127.1, 127.4, 128.0, 132.4, 136.7, 138.2, 141.2, 145.5, 149.7, 157.2 ppm; ES-MS: *m/z*: 907.4291 [*M+H*⁺]; C₆₀H₅₅N₆O₃⁺ requires 907.4330; elemental analysis calcd (%) for C₆₀H₅₄N₆O₃·H₂O C 77.88, H 6.11, N 9.09; found C 77.85, H 5.90, N 9.20.

[Cu₃Cl₆(1)]·CH₃CN·1.5H₂O 7: A solution of tris(4-[2,2',6',2''-terpyridyl]benzyl)cyclotriuaicylene **1** (8 mg, 5.8 μmol) and CuCl₂ (2.8 mg, 11.6 μmol) in acetonitrile (5 mL) was heated at

1 °C min⁻¹ to 130 °C in a 23 mL Parr acid digestion vessel. The solution was kept at this temperature for 48 h; before cooling at 0.1 °C min⁻¹ to room temperature to give very small green crystals of **7** (4.2 mg, 41%). IR (solid state): $\tilde{\nu}$ = 788, 1020, 1085, 1145, 1265, 1403, 1443, 1472, 1512, 1606, 1809, 1930, 2105, 2077, 2929, 3077, 3374, 3567, 3854 cm⁻¹; ES-MS: *m/z*: 1739.16 [[Cu₃Cl₅(1)]⁺/[Cu₆Cl₁₀(1)₂]²⁺], 1512.16 [[Cu₃Cl₅(1)(1-C₂₂H₁₆N₃)₂]²⁺], 1283.18 [[Cu₄Cl₆(1-C₂₂H₁₆N₃)₂]²⁺]/[Cu₂Cl₃(1-C₂₂H₁₆N₃)₂]²⁺], 852.11 [[Cu₃Cl₄(1)]²⁺]; elemental analysis calcd (%) for Cu₃C₉₂H₇₂O₆N₁₀Cl₆·8H₂O: C 56.35, H 4.52, N 7.14; found: C 55.9, H 4.05, N 6.35.

[Ag₄(2)₄](BF₄)₄ 8: A solution of AgBF₄ (5 mg, 25 μmol) in MeCN (few drops) was added to a solution of **2** (11 mg, 13 μmol) in 2,2,2-trifluoroethanol (4 mL). Slow evaporation of the solvent gave crystals of **8** (8 mg, 60%) which, after crystals were selected for X-ray analysis, were filtered and dried in vacuo. IR (solid state): $\tilde{\nu}$ = 485, 519, 555, 585, 622, 660, 746, 763, 781, 827, 880, 914, 929, 943, 1001, 1085, 1141, 1187, 1213, 1276, 1349,

Table 1. Details of data collections and structure refinements for complexes 7–14.

	7	8	9	10
formula	C ₉₂ H ₇₅ Cl ₆ Cu ₃ N ₁₀ O _{7.5}	C ₂₁₆ H ₁₈₀ Ag ₄ B ₄ F ₁₆ N ₁₂ O ₂₄	C ₆₂ H ₅₉ F ₁₂ N ₅ O ₁₁	C ₅₆ H ₄₈ N ₄ O ₆
<i>Mr</i>	1843.94	4106.44	1250.12	872.98
crystal size [mm]	0.13 × 0.03 × 0.02	0.07 × 0.06 × 0.6	0.30 × 0.12 × 0.12	0.12 × 0.07 × 0.06
crystal system	triclinic	tetragonal	monoclinic	monoclinic
space group	<i>P</i> $\bar{1}$	<i>I</i> $\bar{4}$	<i>C</i> 2/ <i>c</i>	<i>P</i> 2 ₁ / <i>c</i>
<i>a</i> [Å]	12.8526(13)	18.5832(9)	37.637(4)	15.1168(8)
<i>b</i> [Å]	17.5353(17)	18.5832(9)	21.344(2)	15.0928(8)
<i>c</i> [Å]	21.026(2)	32.178(3)	16.9385(16)	18.9700(10)
α [°]	103.490(1)	90	90	90
β [°]	104.237(1)	90	96.731(1)	96.457(1)
γ [°]	92.446(1)	90	90	90
<i>V</i> [Å ³]	4441.3(8)	11 112.2(14)	13 513(2)	4300.6(4)
<i>Z</i>	2	2	8	4
ρ_{calcd} [g cm ⁻³]	1.379	1.227	1.229	1.348
μ [cm ⁻¹]	0.953	0.423	0.106	0.088
θ range [°]	3.69–25.0	1.27–17.82	3.63–26.0	1.69–22.53
data collected	2379	9792	38 186	27 759
unique data, <i>R</i> _{int}	11 025, 0.056	3702, 0.0568	9338, 0.0657	6068, 0.0656
obs. data [<i>I</i> > 2 σ (<i>I</i>)]	6806	3032	6124	4690
no. parameters	1066	258	860	776
<i>R</i> _{<i>j</i>} [obs. data]	0.0824	0.0579	0.1082	0.0460
<i>wR</i> ₂ [all data]	0.2860	0.1624	0.3038	0.1265
GOF	1.031	1.087	1.825	1.027
	11	12	13	14
formula	C ₃₈ H ₃₉ AgN ₇ O ₁₀ Re	C ₆₉ H ₇₄ AgF ₆ N ₆ O ₁₀ Sb	C _{63.25} H ₅₉ N ₄ O _{7.25}	C ₆₆ H ₆₆ N ₆ O ₅
<i>Mr</i>	1047.83	1490.96	991.14	1023.25
crystal size [mm]	0.12 × 0.08 × 0.02	0.48 × 0.03 × 0.03	0.51 × 0.03 × 0.03	0.32 × 0.28 × 0.09
crystal system	triclinic	triclinic	monoclinic	triclinic
space group	<i>P</i> $\bar{1}$	<i>P</i> $\bar{1}$	<i>P</i> 2/ <i>c</i>	<i>P</i> $\bar{1}$
<i>a</i> [Å]	8.9251(6)	14.2674(11)	31.8023(17)	11.7202(2)
<i>b</i> [Å]	15.0298(9)	15.0917(12)	9.7186(5)	14.6869(2)
<i>c</i> [Å]	15.2006(9)	16.9138(13)	17.5642(9)	17.4095(3)
α [°]	87.473(4)	111.868(4)	90	77.922(1)
β [°]	76.674(4)	100.442(4)	92.309(3)	77.243(1)
γ [°]	83.130(4)	90.440(4)	90	71.433(1)
<i>V</i> [Å ³]	1969.6(2)	3312.5(4)	5424.2(5)	2739.20(8)
<i>Z</i>	2	2	4	2
ρ_{calcd} [g cm ⁻³]	1.767	1.495	1.214	1.241
μ [cm ⁻¹]	3.634	0.783	0.080	0.079
θ range [°]	1.36–27.42	2.03–25.0	1.28–27.50	3.68–27.51
data collected	45 308	49 406	102 003	69 799
unique data, <i>R</i> _{int}	8748, 0.0417	11 641, 0.0595	12 466, 0.0912	12 515, 0.0707
obs. data [<i>I</i> > 2 σ (<i>I</i>)]	6806	7443	5853	8820
no. parameters	518	813	758	737
<i>R</i> _{<i>j</i>} [obs. data]	0.0325	0.0692	0.1103	0.0707
<i>wR</i> ₂ [all data]	0.0806	0.2216	0.3861	0.2263
GOF	1.096	1.013	1.222	1.034

1378, 1399, 1444, 1465, 1479, 1507, 1571, 1599, 1963, 2866, 2935, 3066, 3527 cm⁻¹; ES-MS: *m/z*: 1965.50 [[Ag₂(2)₂](BF₄)⁺], 1771.60 [[Ag(2)₂]⁺], 940.25 [[Ag(2)]⁺]; elemental analysis calcd (%) for C₃₄H₄₅N₃O₆BF₄Ag·1.5CF₃CH₂OH: C 58.28, H 4.24, N 3.57; found C 58.7, H 4.4, N 3.7.

[Ag(4)]·ReO₄·CH₃CN 11: A solution of AgReO₄ (33 mg, 0.092 mmol) in MeCN (1 mL) was added to a solution of **4** (60 mg, 0.092 mmol) in hot MeCN (25 cm³). Slow evaporation of the solvent gave crystals of **11** (62 mg, 67%), which were filtered off, washed with diethyl ether and dried in vacuo. IR (solid state): $\tilde{\nu}$ = 3129, 2927, 2847, 1611, 1509, 1464, 1424, 1396, 1343, 1325, 1265, 1239, 1210, 1182, 1144, 1084, 1039, 1023, 1006, 945, 903, 861, 829, 794, 730, 653, 616, 585, 535 cm⁻¹; elemental analysis calcd (%) for AgC₃₆H₃₆N₆O₁₀Re: C 42.95, H 3.60, N 8.35; found C 42.50, H 4.05, N 7.95.

[Ag(5)]·SbF₆·3DMF·H₂O 12: Diethylether was allowed to slowly diffuse into a solution of **5** (6 mg, 6.6 μmol) and AgSbF₆ (2.5 mg, 10 μmol) in dimethylformamide (1 mL) giving crystals of **12** (5.9 mg, 71%) after seven weeks. IR (solid state): $\tilde{\nu}$ = 777, 1085, 1144, 1218, 1258, 1346, 1396, 1470, 1508, 1606, 2864, 2930, 3588, 3635 cm⁻¹; elemental analysis calcd (%) for C₆₉H₇₄AgF₆N₆O₁₀Sb: C 55.58, H 5.00, N 5.64; found C, 55.80; H, 4.20, N 3.30.

X-ray crystallography: Crystals were mounted under oil on a glass fibre and X-ray diffraction data collected at 150(1) K with either MoK_α radiation (λ = 0.71073 Å) by using a Bruker Nonius X-8 diffractometer with ApexII detector and FR591 rotating anode generator; or with synchrotron radiation at STFC Daresbury laboratory station 16.2SMX (complexes **7** and **9**, λ = 0.7977 Å) or station 9.8 (complex **10**, λ = 0.6939 Å) by using a Bruker D8 diffractometer fitted with an ApexII detector. Data sets were corrected for absorption using a multi-scan method, and structures were solved by direct methods using SHELXS-97^[37] and refined by full-matrix least squares on F^2 by SHELXL-97,^[38] interfaced through the program X-Seed.^[39] In general, all non-hydrogen atoms were refined anisotropically and hydrogen atoms were included as invariants at geometrically estimated positions, unless specified otherwise in additional details below. Details of data collections and structure refinements are given in Table 1. CCDC 692569 (**7**), 692570 (**8**), 692571 (**9**), 692572 (**10**), 692573 (**11**), 692574 (**12**), 692575 (**13**), and 692576 (**14**) contain the supplementary crystallographic data for this paper. These data can be obtained free of charge from The Cambridge Crystallographic Data Centre via www.ccdc.cam.ac.uk/data_request/cif.

Complex **7** solvent positions were refined at low occupancy and H positions excluded from refinement. Crystals of complex **8** did not diffract to high angles and there was insufficient data for a fully anisotropic refinement, hence only the Ag position was refined anisotropically. One aromatic group was given a rigid body refinement. For both complexes **8** and **9** there was significant void space and diffuse residual electron density, which could not be accurately modelled, hence the SQUEEZE procedure of PLATON was employed.^[29] For complex **9** the hydrogen atoms on a solvent water molecule were fully refined. For complex **10** the hydrogen atoms were fully refined aside from those of solvent molecules. For complex **12** the disordered solvent molecules were refined isotropically and some hydrogen atoms excluded from the model. Complexes **12**, **13**, **14** were all refined with some pyridyl groups showing disorder across two positions, and for complex **14** C/N disorder of some pyridyl groups.

Acknowledgements

The authors would like to acknowledge the EPSRC and University of Leeds for their financial support of this research. The authors thank STFC Daresbury laboratory for access to micro-diffraction facilities, and Martin Huscroft and Ian Blakeley for microanalysis.

- [1] For a review see A. Collet, *Tetrahedron* **1987**, *43*, 5725–5759.
 [2] D. Felder, B. Heinrich, D. Guillon, J.-F. Nicoud, J.-F. Nierengarten, *Chem. Eur. J.* **2000**, *6*, 3501–3507.

- [3] H. A. Fogarty, P. Berthault, T. Brotin, G. Huber, H. Desvaux, J.-P. Dutasta, *J. Am. Chem. Soc.* **2007**, *129*, 10332–10333.
 [4] R. M. Fairchild, K. T. Holman, *J. Am. Chem. Soc.* **2005**, *127*, 16364–16365.
 [5] D. Bardelang, F. Camerel, R. Ziessel, M. Schmutz, M. J. Hannon, *J. Mater. Chem.* **2008**, *18*, 489–494.
 [6] S. Zhang, L. Echegoyen, *J. Am. Chem. Soc.* **2005**, *127*, 2006–2011; J. A. Gawenis, K. T. Holman, J. L. Atwood, S. S. Jurisson, *Inorg. Chem.* **2002**, *41*, 6028–6031.
 [7] E. Huerta, G. A. Metselaar, A. Fragoso, E. Santos, C. Bo, J. de Mendoza, *Angew. Chem.* **2007**, *119*, 206–209; *Angew. Chem. Int. Ed.* **2007**, *46*, 202–205.
 [8] Z. Zhong, A. Ikeda, S. Shinkai, S. Sakamoto, K. Yamaguchi, *Org. Lett.* **2001**, *3*, 1085–1087.
 [9] a) C. J. Sumby, M. J. Hardie, *Angew. Chem.* **2005**, *117*, 6553–6557; *Angew. Chem. Int. Ed.* **2005**, *44*, 6395–6399; b) C. J. Sumby, J. Fisher, T. J. Prior, M. J. Hardie, *Chem. Eur. J.*, **2006**, *12*, 2945–2959.
 [10] C. J. Sumby, M. J. Carr, A. Franken, J. D. Kennedy, C. A. Kilner, M. J. Hardie, *New J. Chem.* **2006**, *30*, 1390–1396.
 [11] A. Westcott, J. Fisher, L. P. Harding, P. Rizkallah, M. J. Hardie, *J. Am. Chem. Soc.* **2008**, *130*, 2950–2951.
 [12] T. K. Ronson, J. Fisher, L. P. Harding, M. J. Hardie, *Angew. Chem.* **2007**, *119*, 9244–9246; *Angew. Chem. Int. Ed.* **2007**, *46*, 9086–9088.
 [13] see for example a) G. I. Birnbaum, D. D. Klug, J. A. Ripmeester, J. S. Tse, *Can. J. Chem.* **1985**, *63*, 3258–3263; b) J. W. Steed, H. Zhang, J. L. Atwood, *Supramol. Chem.* **1996**, *7*, 37–45.
 [14] a) B. T. Ibragimov, K. K. Makhkamov, K. M. Beketov, *J. Indian Acad. Wood Sci. J. Incl. Phenom. Macro. Chem.* **1999**, *30*, 583–593; b) M. R. Caira, A. Jacobs, L. R. Nassimbeni, *Supramol. Chem.* **2004**, *16*, 337–342; c) R. Ahmad, M. J. Hardie, *Supramol. Chem.* **2006**, *18*, 29–38.
 [15] M. J. Hardie, R. M. Mills, C. J. Sumby, *Org. Biomol. Chem.* **2004**, *2*, 2958–2964.
 [16] a) A. Collet, J. Gabard, J. Jacques, M. Cesario, J. Guilhem, C. Pascard, *J. Chem. Soc. Perkin Trans. 1* **1981**, 1630–1638; b) Q.-P. Hu, M.-L. Ma, X.-F. Zheng, J. Reiner, L. Su, *Acta Crystallogr. Sect. E* **2004**, *60*, o1178–o1179.
 [17] a) E. B. Brouwer, K. A. Udachin, G. D. Enright, J. A. Ripmeester, K. J. Ooms, P. A. Halchuk, *Chem. Commun.* **2001**, 565–566; b) M. Makha, M. J. Hardie, C. L. Raston, *Chem. Commun.* **2002**, 1446–1447; c) M. Makha, C. L. Raston, A. N. Sobolev, *Aust. J. Chem.* **2006**, *59*, 260–262.
 [18] a) J. L. Scott, D. R. MacFarlane, C. L. Raston, C. M. Teoh, *Green Chem.* **2000**, *2*, 123–126; b) S.-Q. Wang, G. Zeng, X.-F. Zheng, K. Zhao, *Acta Crystallogr. Sect. A* **2003**, *59*, o1862–o1863.
 [19] J. F. Gallagher, G. Ferguson, V. Böhmer, D. Kraft, *Acta Crystallogr. Sect. C* **1994**, *50*, 73–77.
 [20] see for example a) T. Yamada, G. Fukuhara, T. Kaneda, *Chem. Lett.* **2003**, *23*, 534–535; b) C. Binkowski, F. Hapiot, V. Lequart, P. Martin, E. Monflier, *Org. Biomol. Chem.* **2005**, *3*, 1129–1133; c) T. Haino, M. Yanase, Y. Fukazawa, *Tetrahedron Lett.* **2005**, *46*, 14411–14414; d) D. Bardelang, L. Charles, J.-P. Finet, L. Jicsinszky, H. Karoui, S. R. A. Marque, V. Monnier, A. Rockenbauer, R. Rosas, P. Tordo, *Chem. Eur. J.* **2007**, *13*, 9344–9354.
 [21] S. Cecillon, A. Lazar, O. Danylyuk, K. Suwinska, B. Rather, M. J. Zaworotko, A. W. Coleman, *Chem. Commun.* **2005**, 2442–2444.
 [22] see for example a) J. Martz, E. Graf, M. W. Hosseini, A. de Cian, N. Kyritsakas-Gruber, *C. R. Chim.* **2002**, *5*, 481–486; b) S. Pappalardo, V. Villari, S. Slovak, Y. Cohen, G. Gattuso, A. Notti, A. Pappalardo, I. Pisagatti, M. F. Parisi, *Chem. Eur. J.* **2007**, *13*, 8164–8173.
 [23] a) M. J. Hardie, C. J. Sumby, *Inorg. Chem.* **2004**, *43*, 6872–6874; b) C. J. Sumby, M. J. Hardie, *Cryst. Growth Des.* **2005**, *5*, 1321–1324.
 [24] C. Garcia, J. Malthête, A. Collet, A. *Bull. Soc. Chim. Fr.* **1993**, *130*, 93–95.
 [25] a) A. Gautier, J.-C. Mulatier, J. Crassous, J.-P. Dutasta, *Org. Lett.* **2005**, *7*, 1207–1210; b) J. A. Gawenis, K. T. Holman, J. L. Atwood, S. S. Jurisson, *Inorg. Chem.* **2002**, *41*, 6028–6031; c) O. Reynes, F. Maillard, J.-C. Moutet, G. Royal, E. Saint-Aman, G. Stanciu, J.-P. Dutasta, I. Gosse, J.-G. Mulatier, *J. Organomet. Chem.* **2001**, 637–

- 639, 356–363; d) K. T. Holman, G. W. Orr, J. W. Steed, J. L. Atwood, *Chem. Commun.* **1998**, 2109–2110; e) G. Matouzenko, G. Veriot, J.-P. Dutasta, A. Collet, J. Jordanov, F. Varret, M. Perrin, S. Lecocq, *New J. Chem.* **1995**, *19*, 881–885.
- [26] a) D. S. Bohle, D. J. Stasko, *Chem. Commun.* **1998**, 567–568; b) C. J. Sumbly, K. C. Gordon, T. J. Walsh, M. J. Hardie, *Chem. Eur. J.* **2008**, *14*, 4415–4425.
- [27] a) J. A. Wytko, J. Weiss, *J. Inclusion Phenom. Mol. Recognit. Chem.* **1994**, *19*, 207–225; b) J. A. Wytko, C. Boudon, J. Weiss, M. Gross, *Inorg. Chem.* **1996**, *35*, 4469–4477; c) D. S. Bohle, D. J. Stasko, *Inorg. Chem.* **2000**, *39*, 5768–5770.
- [28] D. A. McMorrán, P. J. Steel, *Chem. Commun.* **2002**, 2120–2121.
- [29] J. D. Crowley, A. J. Goshe, I. M. Steele, B. Bosnich, *Chem. Eur. J.* **2004**, *10*, 1944–1955.
- [30] a) A. J. Amoroso, J. C. Jeffery, P. L. Jones, J. A. McCleverty, P. Thornton, M. D. Ward, *Angew. Chem.* **1995**, *107*, 1577–1580; *Angew. Chem. Int. Ed. Engl.* **1995**, *34*, 1443–1446; b) R. L. Paul, A. J. Amoroso, P. L. Jones, S. M. Couchman, Z. R. Reeves, L. H. Rees, J. C. Jeffery, J. A. McCleverty, M. D. Ward, *J. Chem. Soc. Dalton Trans.* **1999**, 1563–1568; c) S. Hiraoka, T. Yi, M. Shiro, M. Shionoya, *J. Am. Chem. Soc.* **2002**, *124*, 14510–14511; d) M. Albrecht, I. Janser, S. Meyer, P. Weis, R. Fröhlich, *Chem. Commun.* **2003**, 2854–2855; e) R. M. Yeh, J. Xu, G. Seeber, K. N. Raymond, *Inorg. Chem.* **2005**, *44*, 6228–6239; f) T. D. Hamilton, D.-K. Buèar, L. R. MacGillivray, *Chem. Commun.* **2007**, 1603–1604.
- [31] M. Albrecht, I. Janser, S. Burk, P. Weis, *Dalton Trans.* **2006**, 2875–2880.
- [32] a) C. Brückner, R. E. Powers, K. N. Raymond, *Angew. Chem.* **1998**, *110*, 1937–1940; *Angew. Chem. Int. Ed.* **1998**, *37*, 1837–1839; b) D. L. Caulder, C. C. Brückner, R. E. Powers, S. König, T. N. Parac, J. A. Leary, K. N. Raymond, *J. Am. Chem. Soc.* **2001**, *123*, 8923–8938; c) R. W. Saalfrank, H. Glaser, B. Demleiter, F. Hampel, M. M. Chowdhry, V. Schünemann, A. X. Trautwein, G. B. M. Vaughan, R. Yeh, A. V. Davis, K. N. Raymond, *Chem. Eur. J.* **2002**, *8*, 493–497.
- [33] A. K. Spek, *Acta Crystallogr. Sect. A* **1990**, *46*, c34–c34.
- [34] T. Brotin, T. Devic, A. Lesage, L. Emsley, A. Collet, *Chem. Eur. J.* **2001**, *7*, 1561–1573.
- [35] S. Juliá, C. Martínez-Martorell, J. Elguero, *Heterocycles* **1986**, *24*, 2233–2237.
- [36] X. Zeng, A. S. Batsanov, M. R. Bryce, *J. Org. Chem.* **2006**, *71*, 9589–9594.
- [37] G. M. Sheldrick, *Acta Crystallogr. A* **1990**, *46*, 467–473.
- [38] G. M. Sheldrick, *SHELXL-97*, University of Göttingen, Göttingen, Germany, **1997**.
- [39] L. J. Barbour, *Supramol. Chem.* **2003**, *1*, 189–191.

Received: June 25, 2008
Published online: October 1, 2008